Quantification of diffuse myocardial fibrosis using CMR extracellular volume fraction and serum biomarkers of collagen turnover with histologic quantification as standard of reference

C. Foussier, P.A. Barral, M. Jerosh-Herold, V. Gariboldi, Stanislas Rapacchi, A. Gallon, A. Bartoli, Z. Bentatou, Maxime Guye, Monique Bernard, et al.

Version of Record: https://www.sciencedirect.com/science/article/pii/S2211568420301893
Manuscript_5dabae22f3c2cb4209e2106f222f2b46

Quantification of diffuse myocardial fibrosis using CMR extracellular volume fraction and serum biomarkers of collagen turnover with histologic quantification as standard of reference

Short title:

Quantification of diffuse myocardial fibrosis by CMR extracellular volume fraction

Authors

C. FOUSSIER [a, b, #, *]

P.A. BARRAL [a, b, #]

M. JEROSH HEROLD [c],

V. GARIBOLDI [d]

S. RAPACCHIi [b]

A. GALLON [a]

A. BARTOLI [a]

Z. BENTAMOU [b]

M. GUYE [b]

M. BERNARD [b, e]

A. JACQUIER [a, b*]

#CF and PAB contributed equally to this study.

Affiliations

[a] : Department of Radiology, Hôpital de la Timone, 13385 Marseille, France.

[b] : UMR CNRS 7339, Aix-Marseille University, 13385 Marseille, France; Centre de Résonance Magnétique Biologique et Médicale, Hôpital de la Timone, AP-HM, 13385 Marseille cedex 05, France

[c] : Non-Invasive Cardiovascular Imaging Section, Brigham and Women's Hospital, Boston, MA 02215, USA.

[d] : Department of Heart Surgery, Hôpital de la Timone, 13385 Marseille, cedex 05, France.

[e] : Aix-Marseille Univ, CNRS, CRMBM, 13000 Marseille, France

*Corresponding author : Alexis.JACQUIER@ap-hm.fr

Abstract

Purpose: To compare the assessment of diffuse interstitial myocardial fibrosis in valvular diseases using cardiac magnetic resonance (CMR) extracellular volume fraction (ECV) quantification and serum biomarkers of collagen turnover using results of myocardial biopsy as standard of reference.

Materials and methods: This prospective monocentric study included consecutive patients before aortic valvular replacement. All patients underwent *i*), 1.5T CMR with pre and post contrast T_1 mapping sequence and ECV computation *ii*), serum quantification of matrix metalloproteinases (MMPs) and tissue inhibitor of metalloproteinases (TIMPs) and *iii*), myocardial biopsies were collected during surgery to assess collagen volume fraction (CVF). Patients with coronary artery disease were excluded. Correlation between native T1, ECV, CVF and serum biomarkers were assessed using Pearson correlation test. Agreement between basal anteroseptal ECV with global ECV was assessed using Bland-Altman test.

Results: Twenty-one patients, 16 with aortic stenosis and 5 with aortic regurgitation were included. There were 12 men and 9 women with a mean age of 74.1 ± 6.8 (SD) years (range: 32 - 84 years). Mean global ECV value was 26.7 ± 2.7 (SD) % (range: 23.4 - 32.5%) and mean CVF value was 12.4 ± 9.7 % (range: 3.2 - 25.7%). ECV assessed at the basal anteroseptal segment correlated moderately with CVF (r = 0.6; P = 0.0026). There was a strong correlation and agreement between basal anteroseptal ECV and global ECV, (r = 0.8; P < 0.0001; bias 5.4 ± 6.1 %) but no correlation between global ECV and CVF (r = 0.5; P = 0.10). Global ECV poorly correlated with serum TIMP-1 (r = 0.4, P = 0.037) and MMP-2 (r = 0.4, P = 0.047). No correlation was found between serum biomarkers and basal anteroseptal- ECV or native T1.

Conclusion: In patients with severe aortic valvulopathy, diffuse myocardial fibrosis assessed by anterosepto-basal ECV correlates with histological myocardial fibrosis. Anteroseptobasal ECV strongly correlates with global ECV, which poorly correlates with TIMP-1 and MMP-2, serum biomarkers involved in the progression of heart failure.

Keywords: Cardiac magnetic resonance imaging; Aortic valve stenosis; Myocardial fibrosis; Extracellular volume fraction; T1 mapping

List of abbreviations

AR: aortic regurgitation

AS: aortic stenosis

CITP: C-terminal telopeptide of type 1 collagen

CMR: cardiac magnetic resonance

CVF: collagen volume fraction

ECV: extracellular volume fraction

EDV: end diastolic volume

ESV: end systolic volume

ICC: interobserver correlation coeficient

LGE: late gadolinium-chelate enhancement

LVEF: Left ventricular ejection fraction

MMPs: Matrix metalloproteinases

MMP-2: Matrix metalloproteinases 2

MOLLI: modified "Look-Locker" technique

NYHA: New York Heart Association

PICP: carboxy terminal procollagen type 1 propeptide

PIIINP: N-terminal propeptide of type III procollagen

ROI: region-of-interest

SD: standard deviation

TIMP-1: tissue inhibitor of metalloproteinases 1

Introduction

Diffuse myocardial fibrosis is a pathophysiological process causing the impairment of myocardial function and electrical disorganization in valvulopathies. Progress in cardiac magnetic resonance (CMR) now permits the assessment of diffuse myocardial fibrosis in clinical practice by detecting the expansion of extracellular volume (ECV) using T1-mapping techniques [1]. Aortic valvulopathies are characterized not only by progressive valve dysfunction but also by the left ventricular remodeling response [2]. Valvular disease causes pressure overload of the left ventricle and triggers ventricular remodeling response that maintains myocardial performance for years. However, with time, this process decompensates

to heart failure, heralded clinically by the development of symptoms and adverse events, leading to consideration of aortic valve replacement.

Current guidelines recommend intervention in patients with severe aortic stenosis (AS) and evidence of symptoms related to the valvular disease, but other markers include a reduction in ejection fraction < 50%, an abnormal exercise tolerance test or a rise in brain natriuretic peptide level [3, 4]. Unfortunately, symptoms are often difficult to identify in the elderly comorbid patients encountered in clinical practice, and many of the other changes appear only late in the course of the disease after irreversible myocardial damage has become established. Consequently, there is extensive interest in identifying novel, objective markers of early left ventricular decompensation to optimize the timing of aortic valve replacement. The development of such markers requires to improve understanding of the pathophysiology underlying left ventricular decompensation in AS. Histological studies have suggested that myocardial fibrosis and cell death are both important drivers of this process [5, 6]

Myocardial fibrosis can range from focal replacement fibrosis caused by myocardial infarction to diffuse interstitial fibrosis, characterized by the accumulation of collagen in myocardial interstitial tissue. The serum biomarkers of collagen turnover are based on measuring the circulating molecules of extracellular matrix breakdown or remodeling. Matrix metalloproteinases (MMPs) play pivotal roles in the development of fibrosis by controlling extracellular matrix degradation. The tissue inhibitor of metalloproteinases (TIMPs) inhibits MMPs activity [7]. Several studies have validated the correlation between diffuse interstitial fibrosis and the serum biomarkers of collagen turnover but there is very little in the literature concerning the correlation between serum biomarkers, CMR and the histological measurement of fibrosis [8–12]. The up regulation of MMPs and the inadequate inhibition by TIMPs alters the balance between proteolysis/antiproteolysis resulting in the proliferation of fibroblasts and the progression of diffuse myocardial fibrosis [13].

The purpose of this study was to compare the assessment of diffuse interstitial myocardial fibrosis in aortic valve diseases using extracellular volume fraction (ECV) and serum biomarkers of collagen turnover using results of myocardial biopsy as standard of reference.

Material and methods

Patients

This study was approved by the national ethics committee (ID RCB: 2011-A01395-36 31) and all patients gave their informed consent to participate. We prospectively included all patients with severe AS or aortic regurgitation (AR), referred to our Institution for valvular replacement. Non-inclusion criteria were: history of myocardial infarction, hemodynamic instability requiring catecholamine treatment, liver failure, tumor, renal insufficiency (creatinine clearance < 40 mL/min/1.73 m²), high risk of acute coronary syndrome before CMR, history of allergy to gadolinium chelate, pregnancy, breastfeeding, age lower than 18 years and claustrophobia. Exclusion criteria were refusal to undergo CMR and history of cardiac arrhythmia. During a period of 7 days, all patients underwent CMR for ECV quantification, blood samples for collagen turn over biomarker quantification and surgery with myocardial biopsy. New York Heart Association (NYHA) dyspnea classification was recorded for all patients

CMR imaging and image analysis

All CMR examinations were performed on a 1.5T MR system (Avanto®, Siemens Healthineers) with a 32-channel receiver array. Images were acquired in decubitus position with cardiac gating and inspiration breath-hold. Heart rate and blood pressure were recorded during imaging. CMR protocol included two different sequences:

Steady state free precession cine sequences were performed in the long axis, 4 chambers, 2 chambers, LVOT and short axis to cover the whole LV with the following parameters: slice thickness, 7 mm; field of view, 320 mm; temporal resolution, 28.9 ms; TE/TR, 1.6/3.6 ms; flip angle, 35°; image resolution, 256 × 144 - 222. Images were post-processed to evaluate left-ventricular end diastolic (EDV) and end systolic volume (ESV), myocardial mass and LV ejection fraction (LVEF) using vendor-provided software (Argus®, Siemens Healthineers).

T1 mapping using a modified “Look-Locker” technique (MOLLI) [16] with reconstruction including motion correction, was performed before and 17 min after intravenous injection of 0.2 mmoL/kg of gadoterate meglumine (Dotarem®, Guerbet) with the following parameters: slice thickness, 6 mm; field of view, 360 mm; TE/TR, 1.13/2.26 ms; flip angle, 35°; matrix resolution, 256 × 144 - 222. For pre-contrast T1 mapping a 5 (3) 3

MOLLI acquisition scheme was used, and for the post-contrast map a 4 (1) 3 (1) 2 scheme. Pre and post contrast maps were transferred to a CMR 42 workstation (Circle). ECV was measured directly on the ECV map calculated by the software from pre and post T1 maps. ECV measures were carried out in the 12 segments at the basal (6) and mid (6) myocardial levels. The sub-endocardial and sub-epicardial area were excluded (cut off value, 5%) to avoid partial volume effect with blood or epicardial fat.

A late gadolinium-chelate enhancement (LGE) sequence was acquired 10 min after the beginning of intravenous administration of contrast material with the following parameters TR/TE, 650/1.56 ms; slice thickness, 6 mm; number of slabs, 14 (to encompass the left ventricles in the short axis in one breath-hold); flip angle, 10° ; field of view, 350 × 400 mm; matrix size, 152 × 134; and inversion time, 270 – 325 ms (set to null normal myocardium at the end-diastolic phase).

A qualitative analysis of LGE was performed to detect the presence of LGE and the location of myocardial enhancement. CMR images were anonymized and analyzed by two experienced observers blinded to clinical data (A. J. with 10 years of experience in CMR and C.F. with 2 years of experience in CMR).

Blood sample analysis

Blood samples of two serum tubes (6 mL each) and a heparin plasma tube (6 mL) were taken during the week before aortic valve replacement. Standard bioassays were performed with hematocrit. For specific collagen turnover serum biomarkers, samples were centrifuged within 30 min after the samples were taken. Aliquots were then frozen and stored at - 80 °C. The serum biomarkers measured were: carboxy terminal procollagen type 1 propeptide (PICP), C-terminal telopeptide of type 1 collagen (CITP), N-terminal propeptide of type III procollagen (PIIINP), metalloproteinase matrix 2 (MMP-2), tissue inhibitor of metalloproteinase (TIMP-1), galectin, osteopontin, bone specific alkaline phosphatase, and cardiac troponin 1.

Myocardial biopsies and histological study

At the time of surgery, a biopsy of the interventricular septum was performed using an 18 Gauge needle-biopsy (SuperCore™ Biopsy Instrument, Argon Medical Devices, Inc.). Biopsies were collected from the basal antero septum under direct visual control during the aortic valve replacement procedure, then fixed in 10% buffered formalin and embedded in

paraffin, and finally sliced and stained with collagen-specific picrosirius red. The histological measurements of myocardial fibrosis were limited to one sampling site in the LV and were obtained using a 18G needle biopsy which resulted in small myocardial sampling volumes.

Histopathological analysis was performed blinded to clinical and imaging data. Two pathologists performed histological measurements and one performed twice after a period of one month. With respect to the measurements of histological myocardial fibrosis, the collagen volume fraction (CVF) of myocardium was determined by quantitative morphometry (Cellˆ D, Olympus Soft Imaging Solutions) after exclusion of the subendocardial areas. Fibrosis was quantified on stained sections and expressed as a percentage of area, tagged by picrosirius over total myocardial area (Figure 1).

Statistical analysis

Quantitative variables were expressed as means ± standard deviations (SD) and ranges. Categorical variables were expressed as raw numbers, proportions and percentages. Distribution normality was checked using the Shapiro-Wilk test. Patient characteristics were compared with an Anova test for continuous quantitative data, and with Chi-square test for quantitative discrete data. Correlations were estimated by using the Pearson correlation coefficient once normality had been demonstrated, otherwise the Spearman correlation coefficient was used. Local ECV, to be compared with CVF, was measured within a region-of-interest (ROI) in the basal anteroseptal segment and the ROI location was carefully correlated with the location of the targeted surgical biopsy. Global ECV represented the average of the 12 different ECV measures (6 in the basal segments and 6 in the mid-ventricular segments), and was compared with serum biomarkers. Correlations between ECV, histologic fibrosis and serum biomarker of collagen turnover were assessed by the Pearson correlation coefficient (r). The strength of correlation was classified as weak ($0.2 < r \leq 0.5$), moderate ($0.5 < r \leq 0.8$), strong ($0.8 < r < 1$) and perfect ($r = 1$). Bland-Altman analysis was used to illustrate agreement between basal anteroseptal ECV and global ECV. Intraclass correlation coefficient (ICC) was used to assess inter and intra observer reproducibility for histological measurements and ECV.

Statistical tests were 2-tailed and $P < 0.05$ was considered to indicate a statistically significant difference. All statistical analysis was performed with available software packages (GraphPad Prism, Graph Pad Software, Inc. La Jolla, USA).

Results

Study population

Thirty-one patients were prospectively included from May 2012 to October 2013. 5 patients were excluded from CMR (claustrophobia, 4 and severe arrhythmia, and analysis comparing CMR with blood biomarker were performed on 26 patients. Five patients (all suffering from AS) refused to undergo surgical myocardial biopsy but had the whole protocol, so analysis comparing histology with other parameters were performed on 21 patients. Figure 2 shows the study flow chart.

Patients characteristics are summarized in Table 1. Seventeen patients had severe AS and four patients had severe AR. The mean delay between CMR, serum biomarkers and surgery was 4 ± 1.5 (SD) days (range: 2 - 5 days). Myocardial biopsies were performed without any complications in all patients. Mean global native T1 was 984.3 ± 22.5 ms (range: 922.1 - 1067.3 ms), mean global ECV was 26.7 ± 2.7 (SD) % (range: 23.4 - 32.5%). Mean basal anteroseptal native T1 was 961.2 ± 34.3 (SD) ms (range: 918.4 - 1073.7 ms) and mean basal anteroseptal ECV was 26.1 ± 2.6 (SD) % (range: 23.2 - 30.8%). The mean percentage of CVF was 12.4 ± 9.7 (SD) % (range: 3.2 - 25.7%). No LGE was detected in the interventricular septum, nor in the LV subendocardial layer. Four patients showed subtle areas of LGE on CMR at the insertion points of RV on the LV.

CMR versus CVF

Neither basal anteroseptal native T1 nor global native T1 correlated with CVF (r = 0.22; P = 0.33). A positive moderate correlation was found between basal anteroseptal ECV and CVF (r = 0.65; P = 0.002) (Fig. 3). No significant correlation was found between global ECV and CVF (r = 0.46; P = 0.101. Global ECV strongly correlated with basal anteroseptal ECV (r = 0.79; P < 0.0001)) (Fig. 4). Bland-Altman analysis revealed good agreement between global and basal anteroseptal ECV (Fig. 5). Overall ECV was not significantly greater than basal anteroseptal ECV but showed a larger SD of the mean and segmental ECV value ranged from 21% to 48% considering all measured segments with a positive bias of 0.014 ± 0.017 (SD) %for the difference between global ECV and basal anteroseptal ECV and with a positive bias of 5.37 ± 6.15 (SD) % for the percent of difference between the two measurements.

CMR versus serum biomarkers of collagen turnover

There was no significant correlation between native T1 map and serum biomarkers. Poor correlation was found between overall ECV and TIMP-1 ($r = 0.41$; $P = 0.04$) (Fig. 6) and overall ECV and MMP-2 ($r = 0.39$; $P = 0.04$) (Fig. 7). No significant associations were found between global ECV and the expression of PICP ($P = 0.12$), CITP ($P = 0.72$), Galectin ($P = 0.99$) and PIINP ($P = 0.44$).

Serum biomarkers versus ECV, CVF and clinical data

No correlation was found between the basal anteroseptal ECV or global ECV and these parameters. CITP moderately correlated with EDVi ($r = 0.54$; $P = 0.007$), ESVi ($r = 0.55$; $P = 0.01$) and myocardial mass ($r = 0.47$; $P = 0.02$). PIC-P poorly correlated with EDVi ($r = 0.47$; $P = 0.02$) and ESVi ($r = 0.41$; $P = 0.04$) (Table 2). Galectin, TIMP-1 and MMP-2 did not correlate with these functional parameters. No significant relationship was found between the blood biomarkers and histologic fibrosis.

Reproducibility of measurements

The interobserver reproducibility of the histological measurements (ICC) was 0.80 with a bias of 0 ± 4 (SD) % and the intraobserver reproducibility was 0.89 with a bias of 0 ± 2%. The inter and intraobserver reproducibility for ECV assessment were ICC: 0.61 with a bias of - 0.8 ± 3.6 (SD) % and 0.71 with a bias of - 0.8 ± 3.0 (SD) %.

Discussion

In this study, we found that the basal anteroseptal ECV derived from 1.5 T CMR MOLLI T1 mapping, 17 min after bolus injection of a gadolinium chelate moderately correlates with the magnitude of diffuse interstitial myocardial fibrosis measured by picosirius red staining on histopathological samples taken from patients undergoing valve surgery. In addition, we observed that basal anteroseptal ECV is strongly correlated with global ECV. Finally, global ECV poorly correlated with TIMP-1 and MMP-2 which are known serum biomarkers of collagen turnover.

The global ECV measured in the present study is within the normal range published elsewhere [15]. This was in line with previous publication showing that ECV is slightly increased in patients with valvular disease [16-17]. De Meester et al. included patients with AS and patients with AR and found a mean global ECV of 28.9 ± 5.5 (SD) % and a mean

CVF of 6.1 ± 4.3 (SD) % at 3T [16]. Treibel et al. who included only patients with AS, found a mean global ECV of 28.4 ± 2.4 (SD) % at 1.5T CMR and a mean CVF of 11.5 ± 8.6 (SD) % [17].

In the present study, the histological measurements of myocardial fibrosis were limited to one sampling site in the LV using a 18-Gauge needle biopsy. In AS and valvular regurgitation, the diffuse reactive myocardial fibrosis is more ubiquitous than focal fibrosis [18]. Child et al. demonstrated that ECV values show a significant association with CVF when sampled by septal ROI instead of entire coverage of the midventricular short-axis slice [19]. In fact, diffuse myocardial fibrosis is a heterogeneous process [20]. Myocardial fibrosis is categorized according to distinct patterns: compact, patchy, interstitial and diffuse [21]. These different patterns of fibrosis may not have equivalent arrhythmogenic profiles [22, 23]. LGE is an accurate method of assessing focal replacement fibrosis, but only partially reflects the complete burden of myocardial fibrosis in cases of severe aortic valvulopathy. Nevertheless focal replacement fibrosis, measured by LGE, worsens the prognosis for adverse cardiovascular events in dilated and hypertrophic cardiomyopathy substantially [24, 25]. One the other hand, diffuse myocardial fibrosis, measured by ECV, is also significantly associated with cardiovascular mortality: death, higher hospitalization rate for heart failure, or both. [26]. In the future, more works may be required to assess the heterogeneity of myocardial fibrosis in order to understand precisely which parameters will be the best surrogate markers for myocardial prognosis.

MMPs play a pivotal role in the development of fibrosis by controlling extra cellular matrix degradation [13]. Recent studies have shown that MMPs are not only involved in extra cellular matrix degradation, but also in the progression of heart failure [27]. The cardiac expression of TIMP-1 and TIMP-2 is significantly increased in chronic pressure-overloaded cardiopathy compared with controls and is related to the degree of interstitial fibrosis [7]. Nevertheless propeptide of procollagen which correlates with histologic CVF [9, 10], correlates with excentric and concentric cardiac remodeling in our study. Myocardial fibrosis increases ventricular stiffness and leads to diastolic dysfunction. Zeng et al. showed a link between ECV and diastolic strain rate in diabetic rabbits [28]. Wu et al. showed a correlation between ECV and diastolic function in patients with hypertrophic cardiomyopathy [29]. Furthermore, patients with type 2 diabetes mellitus and normal myocardial systolic strain exhibit increased ECV, which correlates with their glycated hemoglobin level [30]. Our ability to evaluate ECV in a variety of cardiomyopathies may enhance our understanding of the pathogenesis and help better assess prognosis of these conditions. There is a gap that must

be filled before we are able to define the parameters reflecting myocardial fibrosis that could be of clinical interest.

Our study has limitations: Our prospective experimental study was limited to a single center with a relatively small number of patients. One limitation of any radiological vs histological study is the almost unavoidable mismatch between placement of the local ECV's ROI and the biopsy site, which could lead to a possible miscorrelation, particularly with a fine 18-Gauge coaxial biopsy.

In conclusion, concerning severe aortic valvulopathy, diffuse myocardial fibrosis assessed by anterosepto-basal ECV correlates with histological myocardial fibrosis. Anteroseptobasal ECV strongly correlates with global ECV, which poorly correlates to TIMP-1 and MMP-2, serum biomarkers involved in the progression of heart failure. Diffuse myocardial fibrosis remains an inhomogeneous process, incompletely depicted by only ECV analysis.

Ethics approval and consent to participate

This study was approved by the national ethical committee (ID RCB: 2011-A01395-36 31).
All patients gave their informed consent to participate.

Funding

This research received PHRC grant: PHRC N= 2011-A00887-34

Authors' Contributions

Conception / design of the work: AJ, PAB, CF
Acquisition of data: VG, AG, AJ
Interpretation of data: MJH, ZB; AB, SR, AJ, PAB
Dratf and revision: MG, MB, SR, AJ, PAB
All authors substantially modified, read and approved the final manuscript.
All authors agreed both to be personally accountable for the author's own contributions and to ensure that questions related to the accuracy or integrity of any part of the work are appropriately investigated, resolved, and the resolution documented in the literature

Competing Interests

The authors declare that they have no competing interests

References

1. Messroghli DR, Moon JC, Ferreira VM, Grosse-Wortmann L, He T, Kellman P, et al. Clinical recommendations for cardiovascular magnetic resonance mapping of T1, T2, T2* and extracellular volume: a consensus statement by the Society for Cardiovascular Magnetic Resonance (SCMR) endorsed by the European Association for Cardiovascular Imaging (EACVI). J Cardiovasc Magn Reson 2017;19: 75.

2. Dweck MR, Boon NA, Newby DE. Calcific aortic stenosis: a disease of the valve and the myocardium. J Am Coll Cardiol 2012;60: 1854–63.

3. Baumgartner H, Falk V, Bax JJ, De Bonis M, Hamm C, Holm PJ, et al. 2017 ESC/EACTS Guidelines for the management of valvular heart disease. Eur Heart J 2017;38: 2739–91.

4. Nishimura RA, Otto CM, Bonow RO, Carabello BA, Erwin JP, Guyton RA, et al. 2014 AHA/ACC Guideline for the management of patients with valvular heart disease: executive summary: a report of the American College of Cardiology/American Heart Association Task Force on Practice Guidelines. Circulation 2014;129:2440–92.

5. Krayenbuehl HP, Hess OM, Monrad ES, Schneider J, Mall G, Turina M. Left ventricular myocardial structure in aortic valve disease before, intermediate, and late after aortic valve replacement. Circulation 1989;79:744–55.

6. Hein S, Arnon E, Kostin S, Schönburg M, Elsässer A, Polyakova V, et al. Progression from compensated hypertrophy to failure in the pressure-overloaded human heart: structural deterioration and compensatory mechanisms. Circulation 2003;107:984–91.

7. Bonnans C, Chou J, Werb Z. Remodelling the extracellular matrix in development and disease. Nat Rev Mol Cell Biol 2014;15:786–801.

8. Querejeta R, Varo N, López B, Larman M, Artiñano E, Etayo JC, et al. Serum carboxy-terminal propeptide of procollagen type I is a marker of myocardial fibrosis in hypertensive heart disease. Circulation 2000;101:1729–35.

9. Izawa H, Murohara T, Nagata K, Isobe S, Asano H, Amano T, et al. Mineralocorticoid receptor antagonism ameliorates left ventricular diastolic dysfunction and myocardial fibrosis in mildly symptomatic patients with idiopathic dilated cardiomyopathy: a pilot study. Circulation 2005;112:2940–5.

10. Klappacher G, Franzen P, Haab D, Mehrabi M, Binder M, Plesch K, et al. Measuring extracellular matrix turnover in the serum of patients with idiopathic or ischemic dilated cardiomyopathy and impact on diagnosis and prognosis. Am J Cardiol 1995;75:913–8.

11. López B, González A, Querejeta R, Zubillaga E, Larman M, Díez J. Galectin-3 and histological, molecular and biochemical aspects of myocardial fibrosis in heart failure of hypertensive origin. Eur J Heart Fail 2015;17:385–92.
12. López B, González A, Querejeta R, Larman M, Díez J. Alterations in the pattern of collagen deposition may contribute to the deterioration of systolic function in hypertensive patients with heart failure. J Am Coll Cardiol 2006;48:89–96.
13. Polyakova V, Hein S, Kostin S, Ziegelhoeffer T, Schaper J. Matrix metalloproteinases and their tissue inhibitors in pressure-overloaded human myocardium during heart failure progression. J Am Coll Cardiol 2004;44:1609–18.
14. Messroghli DR, Radjenovic A, Kozerke S, Higgins DM, Sivananthan MU, Ridgway JP. Modified Look-Locker inversion recovery (MOLLI) for high-resolution T1 mapping of the heart. Magn Reson Med 2004;52:141–6.
15. Vo HQ, Marwick TH, Negishi K. Pooled summary of native T1 value and extracellular volume with MOLLI variant sequences in normal subjects and patients with cardiovascular disease. Int J Cardiovasc Imaging 2020;36:325–36.
16. de Meester de Ravenstein C, Bouzin C, Lazam S, Boulif J, Amzulescu M, Melchior J, et al. Histological Validation of measurement of diffuse interstitial myocardial fibrosis by myocardial extravascular volume fraction from Modified Look-Locker imaging (MOLLI) T1 mapping at 3 T. J Cardiovasc Magn Reson 2015;17:48.
17. Treibel TA, López B, González A, Menacho K, Schofield RS, Ravassa S, et al. Reappraising myocardial fibrosis in severe aortic stenosis: an invasive and non-invasive study in 133 patients. Eur Heart J 2018;39:699–709.
18. Mewton N, Liu CY, Croisille P, Bluemke D, Lima JAC. Assessment of myocardial fibrosis with cardiovascular magnetic resonance. J Am Coll Cardiol 2011;57:891–903.
19. Child N, Yap ML, Dabir D, Rogers T, Suna G, sandhu banher, et al. T1 values by conservative septal postprocessing approach are superior in relating to the interstitial myocardial fibrosis: findings from patients with severe aortic stenosis. J Cardiovasc Magn Reson 2015;17 49.
20. Kazbanov IV, ten Tusscher KHWJ, Panfilov AV. Effects of heterogeneous diffuse fibrosis on arrhythmia dynamics and mechanism. Sci Rep 2016;6:20835.
21. Nguyen TP, Qu Z, Weiss JN. Cardiac fibrosis and arrhythmogenesis: the road to repair is paved with Perils. J Mol Cell Cardiol 2014;70:83–91.

22. Morita N, Sovari AA, Xie Y, Fishbein MC, Mandel WJ, Garfinkel A, et al. Increased susceptibility of aged hearts to ventricular fibrillation during oxidative stress. Am J Physiol Heart Circ Physiol 2009;297:H1594–605.
23. McDowell KS, Arevalo HJ, Maleckar MM, Trayanova NA. Susceptibility to arrhythmia in the infarcted heart depends on myofibroblast density. Biophys J 2011;101:1307–15.
24. Becker MAJ, Cornel JH, van de Ven PM, van Rossum AC, Allaart CP, Germans T. The prognostic value of late gadolinium-enhanced CMR in nonischemic dilated cardiomyopathy. J Am Coll Cardiol 2018;11:1274–84.
25. Weng Z, Yao J, Chan RH, He J, Yang X, Zhou Y, et al. Prognostic value of LGE-CMR in HCM: a meta-analysis. JACC Cardiovasc Imaging 2016;9:1392–402.
26. Schelbert EB, Piehler KM, Zareba KM, Moon JC, Ugander M, Messroghli DR, et al. Myocardial fibrosis quantified by extracellular volume is associated with subsequent hospitalization for heart failure, death, or both across the spectrum of ejection fraction and heart failure stage. J Am Heart Assoc 2015;4:e002613
27. Spinale FG, Janicki JS, Zile MR. Membrane associated matrix proteolysis and heart failure. Circ Res 2013;112:195–208.
28. Zeng M, Qiao Y, Wen Z, Liu J, Xiao E, Tan C, et al. The association between diffuse myocardial fibrosis on cardiac magnetic resonance T1 mapping and myocardial dysfunction in diabetic rabbits. Sci Rep 2017;7:44937.
29. Wu R, An DA, Shi RY, Chen BH, Jiang M, Bacyinski A, et al. Myocardial fibrosis evaluated by diffusion-weighted imaging and its relationship to 3D contractile function in patients with hypertrophic cardiomyopathy. J Magn Reson Imaging 2018;48:1139-46.
30. Cao Y, Zeng W, Cui Y, Kong X, Wang M, Yu J, et al. Increased myocardial extracellular volume assessed by cardiovascular magnetic resonance T1 mapping and its determinants in type 2 diabetes mellitus patients with normal myocardial systolic strain. Cardiovasc Diabetol 2018; 4: 7.

Figures

Figure 1: Multiparametric fibrosis quantification with CMR and histopathological sample from: A 77-year-old man suffering from severe aortic stenosis (AS) (LGE images are not shown because of normality). The different maps were created with Circle® software (Calgary, Canada). A: Native T1 map (1028 ms), B: Post contrast T1 map (449 ms), C: Extra cellular volume (0.29), D: Collagen volume fraction (14 %).

Figure 2: Study flowchart.

Figure 3: Graph shows correlation between basal anteroseptal extracellular volume (ECV) and collagen volume fraction (CVF) (r = 0.65; P = 0.0026).

Figure 4: Graph shows correlation between global extracellular volume (ECV) and basal anteroseptal extracellular volume (ECV) (r = 0.79; P < 0.0001).

Figure 5: Graph shows Bland-Altman plots for comparison between global extracellular volume (ECV) and basal anteroseptal extracellular volume (ECV). The top and bottom line shows +1.96 standard deviation (SD) and -1.96 SD. Positive bias of 0.0141 (SD of bias 0.0173) for the difference between global ECV and basal anteroseptal ECV and with a positive bias of 5.37% (SD of bias of 6.15%) for the % of difference between the both measures.

Figure 6: Graph shows correlation between global extracellular volume (ECV) and tissue inhibitor of metalloproteinase (TIMP-1) (r = 0.41; P = 0.0378).

Figure 7: Graph shows correlation between global extracellular volume (ECV) and Matrix metalloproteinase 2 (MMP-2) (r = 0.39; P = 0.0475).

Table 1: Patients characteristics.

Table 2: Correlation between functional CMR variables and serum biomarkers in 26 patients.

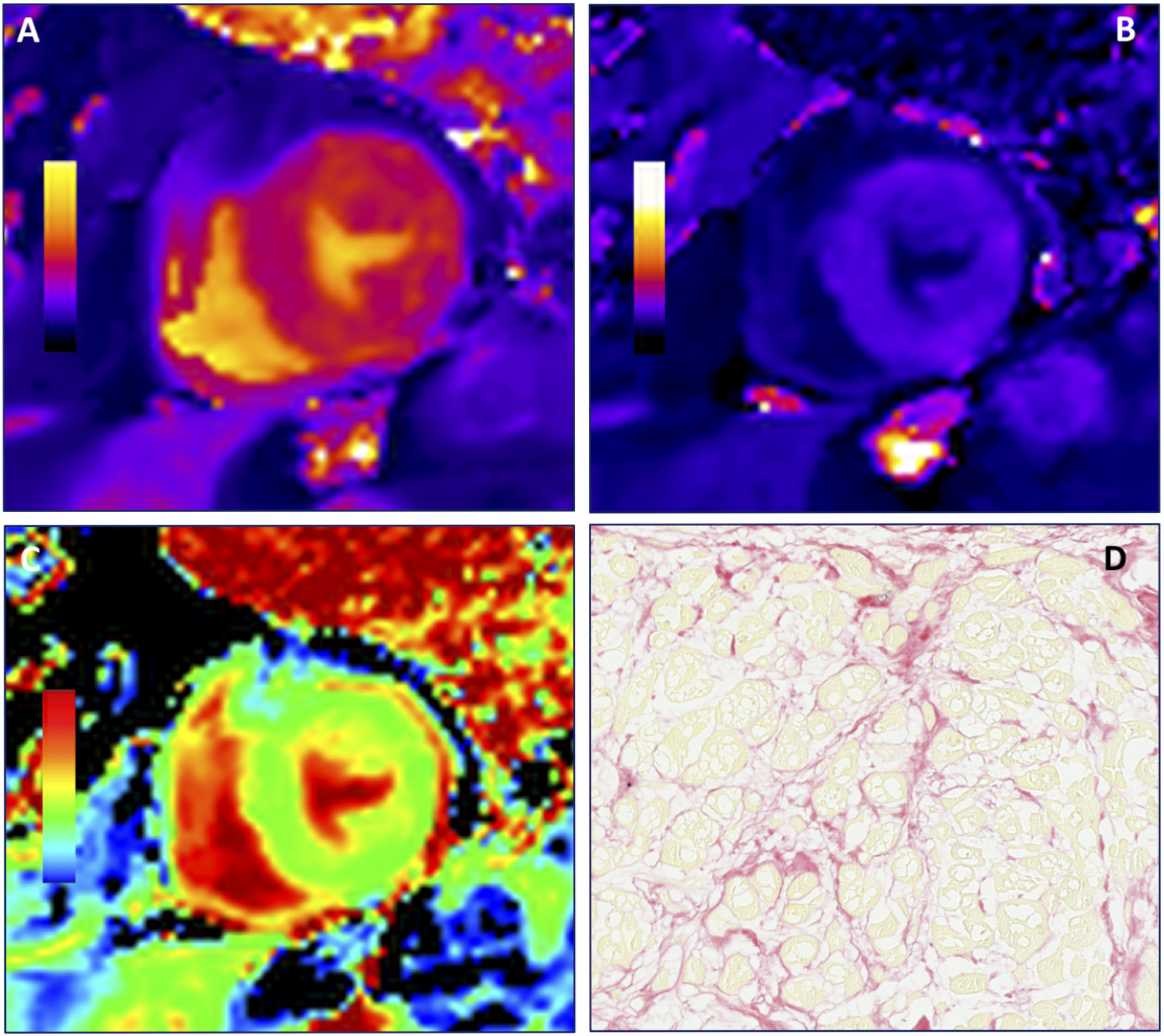
A
B
C
D

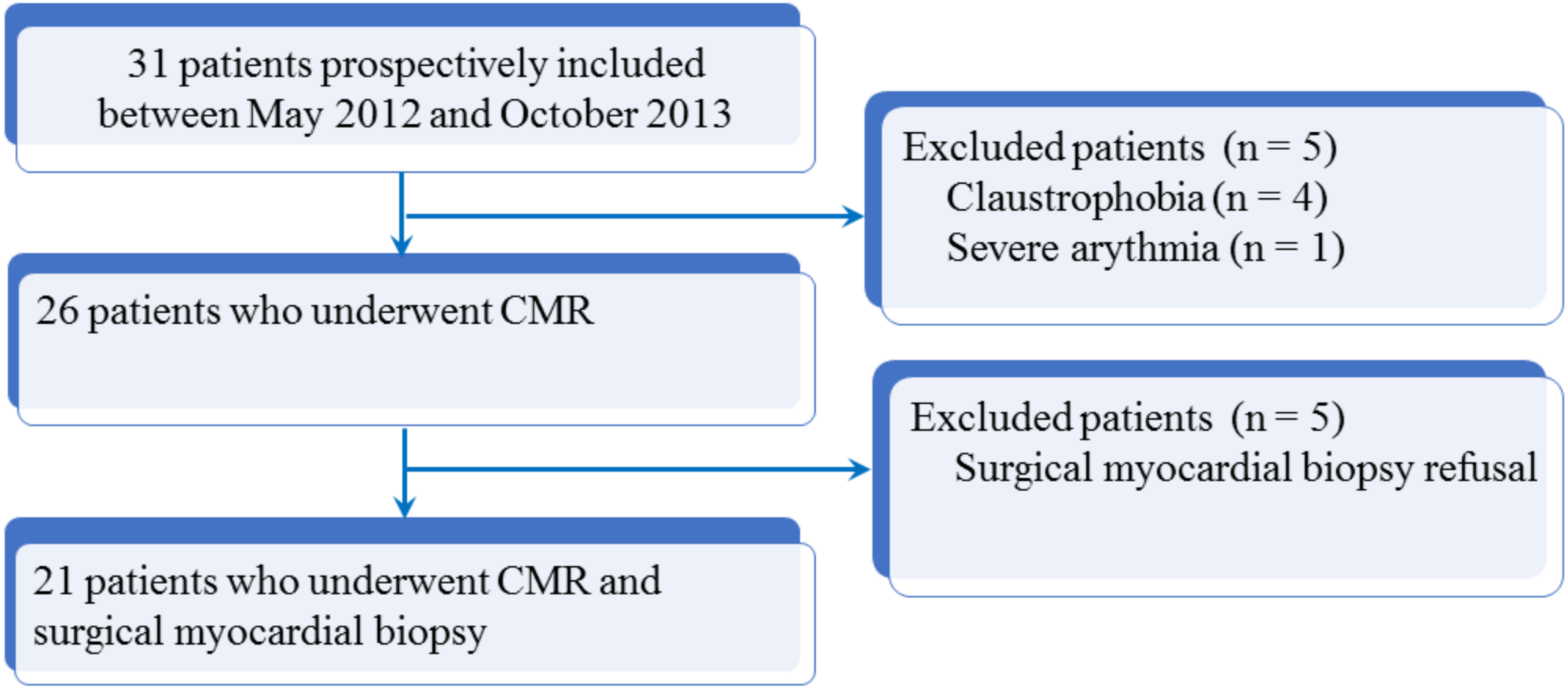
31 patients prospectively included between May 2012 and October 2013
Excluded patients (n = 5)
Claustrophobia (n = 4)
Severe arythmia (n = 1)
26 patients who underwent CMR
Excluded patients (n = 5)
Surgical myocardial biopsy refusal
21 patients who underwent CMR and surgical myocardial biopsy

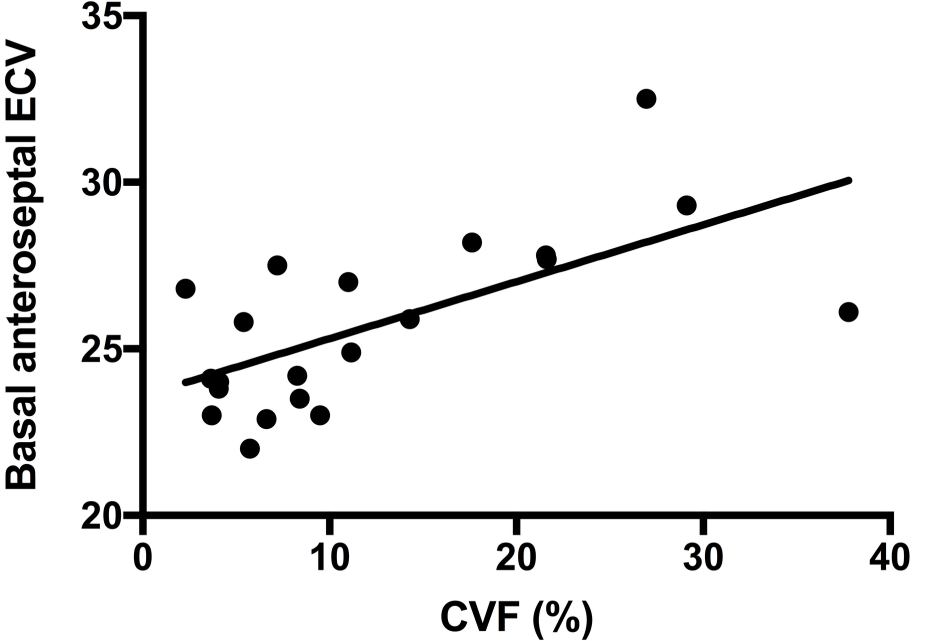
Basal anteroseptal ECV
35
30
25
20
0
10
20
30
40
CVF (%)

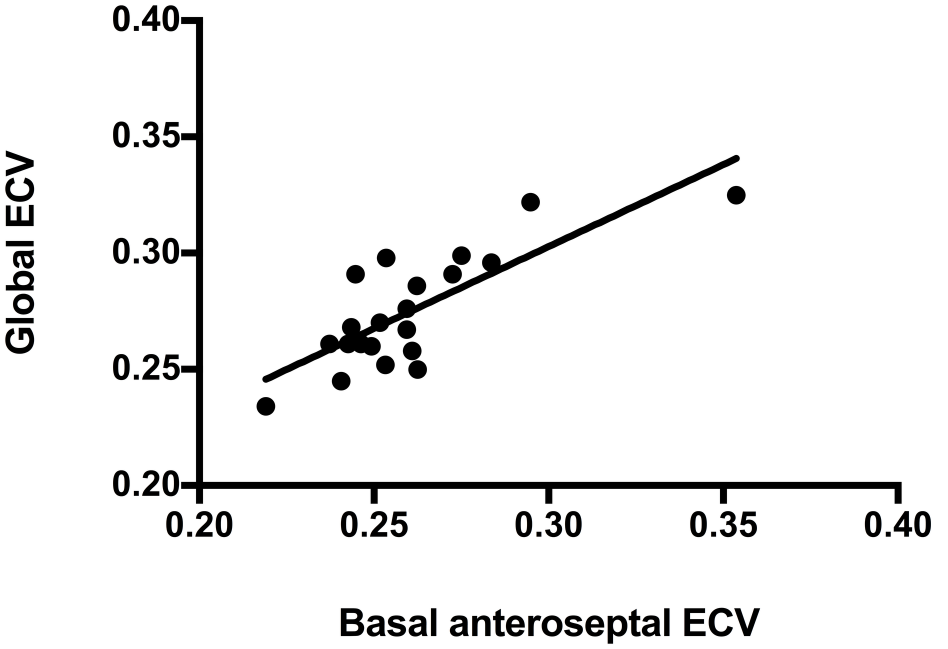
0.40
0.35
0.30
0.25
0.20
Global ECV
0.20
0.25
0.30
0.35
0.40
Basal anteroseptal ECV

Agreement between Global and anteroseptobasal ECV

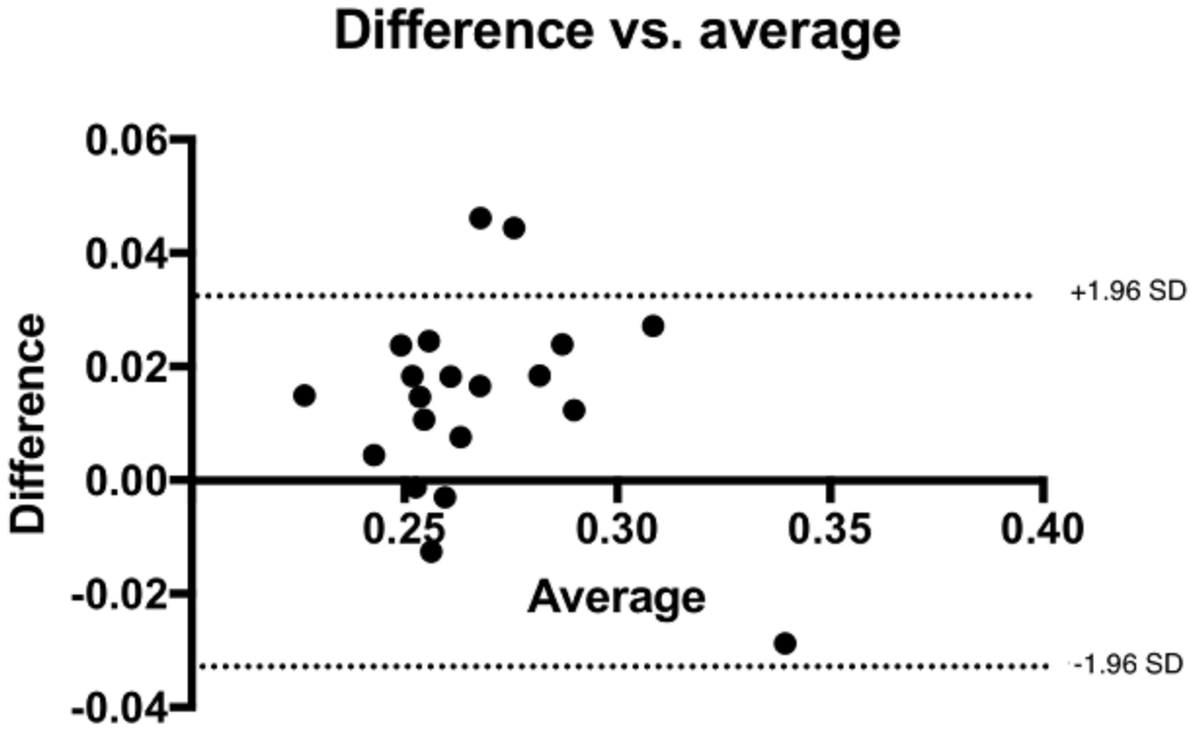

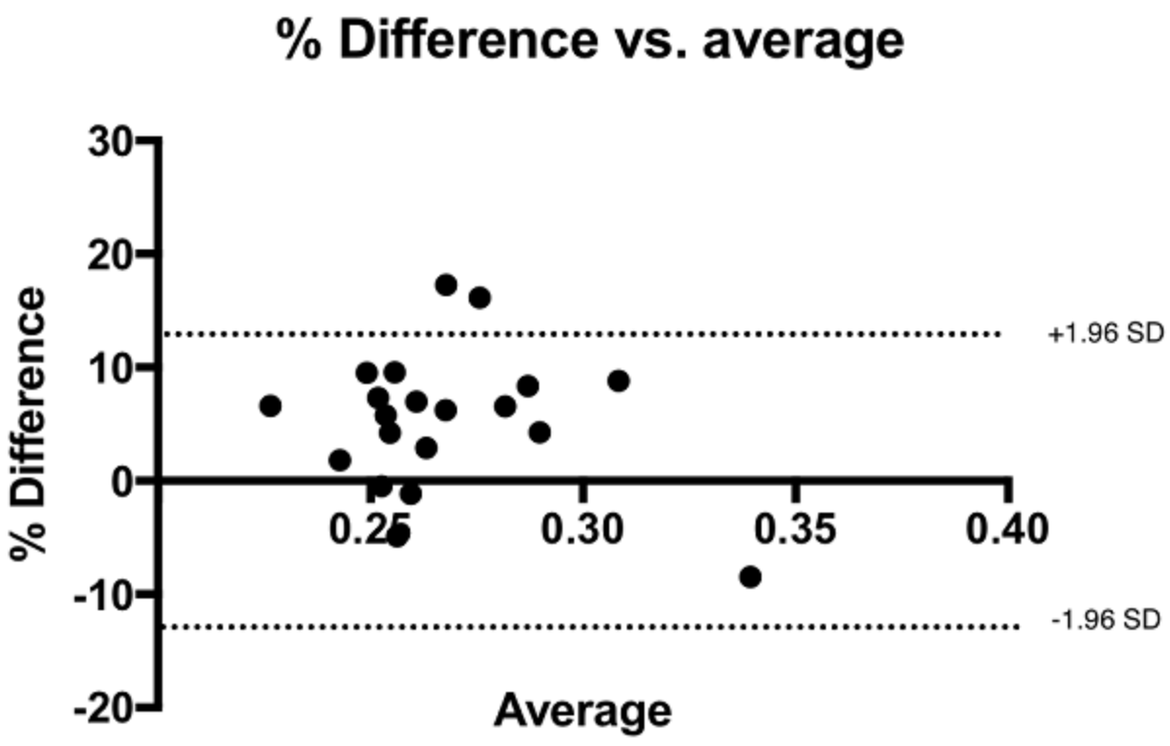

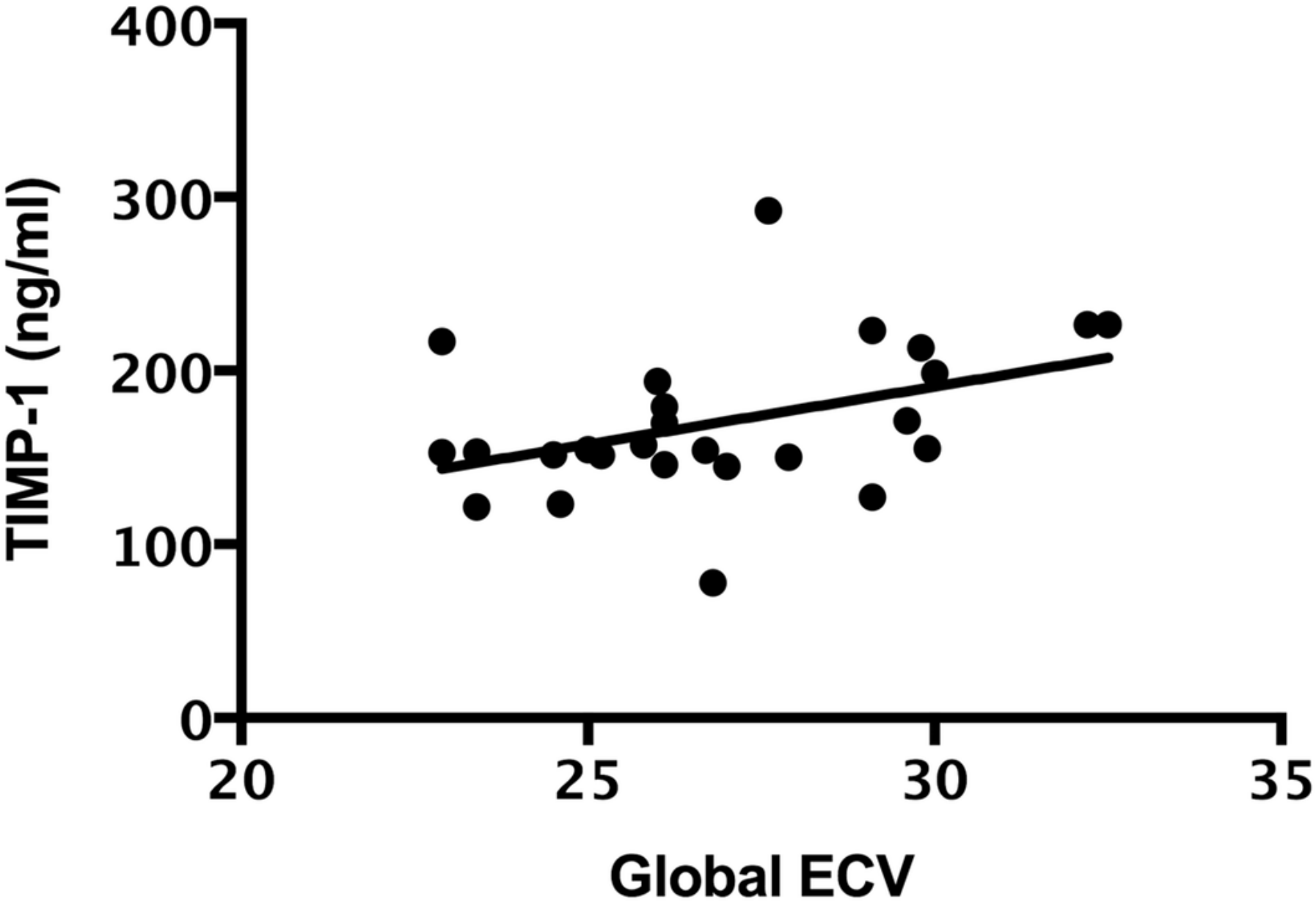
400
300
200
100
0
TIMP-1 (ng/ml)
20
25
30
35
Global ECV

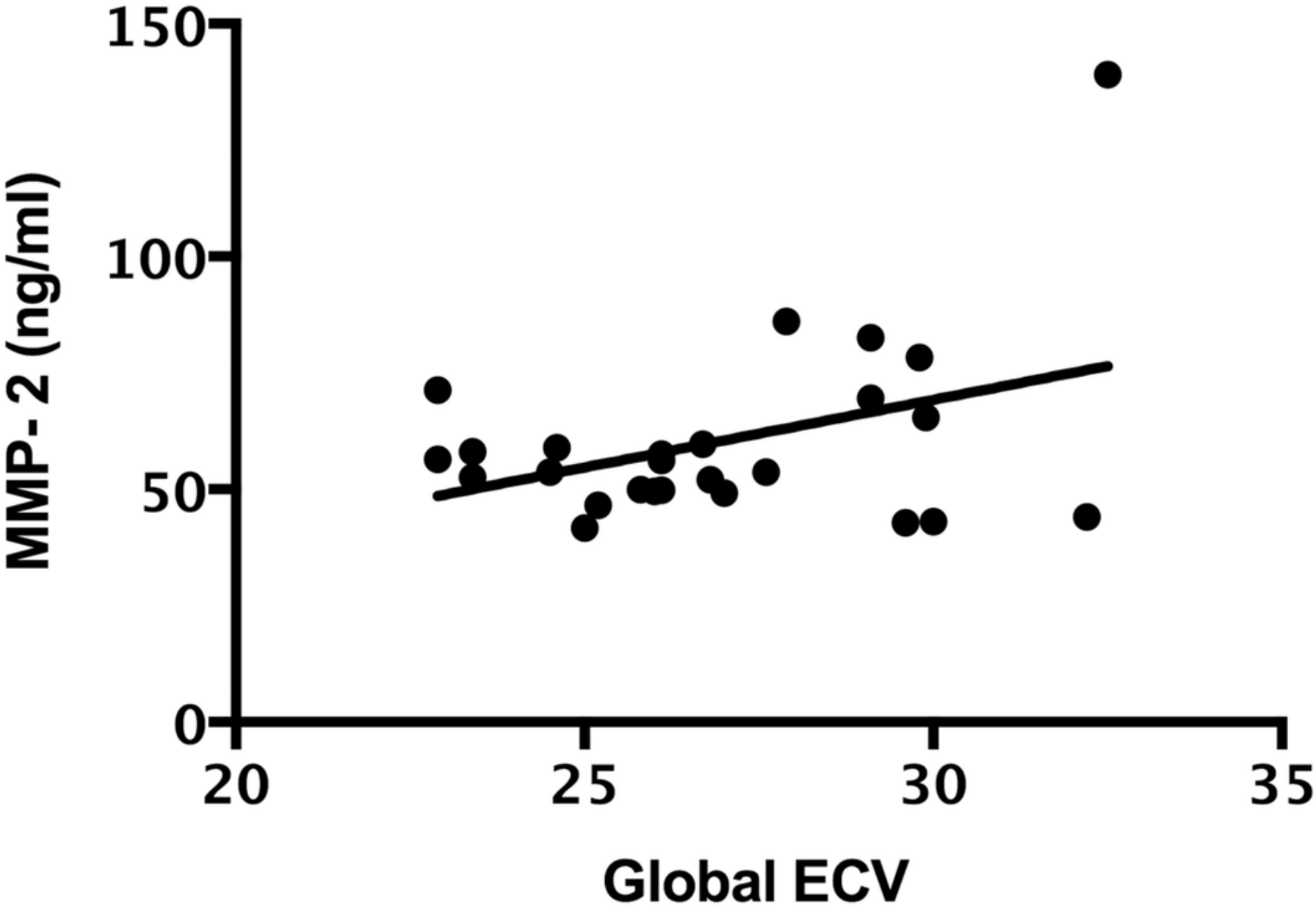
150
100
50
0
MMP- 2 (ng/ml)
20
25
30
35
Global ECV

Valvulopathy	**Aortic stenosis** (n =17)	**Aortic regurgitation** (n = 4)	**All patients** (n =21)
Clinical data			
Age (year)	76.2 ± 6.2 [53 – 84]	65.4 ± 9.8 [32 – 72]	74.1 ± 6.8 [32 – 84]
Male	10 (10/17; 59%)	2 (2/4; 50%)	12 (12/21; 57%)
BMI (kg/m^2)	27.8 ± 4.2 [24 – 40]	25.1 ± 8.7 [22 – 31]	27.2 ± 4.9 [22 – 40]
Heart rate (beats/min)	70.1 ± 8.4 [53 – 92]	71.3 ± 9.4 [56 – 89]	70.3 ± 8.8 [53 – 92]
Hematocrit (%)	40.7 ± 6.3 [36 – 45]	40.4 ± 8.6 [36 – 44]	40.6 ± 7.4 [36 – 45]
NYHA class			
I	2 (2/17; 12%)	2 (2/4; 50%)	2 (2/21; 10%),
II	10 (10/17; 59%)	2 (2/4; 50%)	12 (12/21; 57%),
III	5 (5/17; 29.4%)	0 (0/4; 0%)	7 (7/21; 33%),
IV	0 (0/17; 0%)	0 (0/4; 0%)	0 (0/21; 0%)
CMR parameters			
LV EF (%)	62.5 ± 12.1 [46 – 75]	57.4 ± 10.8 [44 – 70]	61.2 ± 12.2 [44 – 75]
ED volume index (mL/m^2)	67.3 ± 19.5 [35.4 – 106.2]	105.7 ± 25.2 [140.6 – 84.2]	68.1 ± 20.7 [35.4 – 140.6]
ES volume index (mL/m^2)	26.4 ±13.4 [9.5 – 50.2]	44.6 ± 12.4 [27.2 – 56.7]	29.5 ± 17.4 [9.5 – 56.7]
Stroke volume index (mL/m^2)	53.9 ±16.7 [40.2 – 61.4]	61.1 ± 23.4 [39.3 – 78.7]	54.5 ±18.1 [39.8 – 78.7]
LV mass index (g/m^2)	81.2 ± 20.8 [52.9 – 119.2]	84.1 ± 9.9 [69.1 – 9 1.3]	81.7 ± 19.0 [52.9 – 119.2]
Native T1 (ms)	977.5 ± 24.8 [929 – 1035]	1006.5 ± 30.9 [922-1067]	984.3 ± 22.5 [922 – 1067]
Global ECV	25.9 ± 2.6 [22.9 – 32.1]	29.6 ± 3.2 [23.8 - 31.7]	26.7 ± 2.7 [22.9 – 32.1]
Basal anteroseptal ECV	26.0 ± 1.9 [23.2 – 30.8]	26.3 ± 3.7 [23.7 – 30.6]	26.1 ± 2.6 [23.2 – 30.8]
Histology			
CVF (%)	14.1 ± 10.2 [3.2 – 25.7]	6.5 ± 4.8 [3.6 – 9.5]	12.4 ± 9.7 [3.2 – 25.7]

BMI: body mass index; ECV: extracellular volume fraction; LVEF: left ventricular ejection fraction; ED: end-diastolic; ES: end-systolic; LV: left ventricule; CVF: collagen volume fraction

Quantitative data are expressed as means ± standard deviations; numbers in brackets are ranges. Qualitative data are expressed as raw numbers; numbers in parentheses are proportions followed by percentages.

	EDVi (ml/m^2)	ESVi (ml/m^2)	LVMi (g/m^2)	LVEF (%)
Galectin-3 (ng/mL)	r = 0.08; P = 0.56	r = 0.04; P = 0.61	r = -0.15; *P = 0.31*	r = 0.14; P = 0.27
TIMP-1 (ng/mL)	r = 0.17; P = 0.39	r = -0.05; P = 0.57	r = 0.01; P = 0.59	r = 0.21; P = 0.18
MMP-2 (ng/mL)	r = 0.02; P = 0.47	r = 0.12; P = 0.41	r = 0.08; P = 0.37	r = -0.15; P = 0.39
PIC-P (ng/mL)	**r = 0.47; P = 0.02**	**r = 0.41; P = 0.04**	r = 0.161; P = 0.18	r = -0.192; P = 0.40
CITP (µg/L)	**r = 0.54; P = 0.01**	**r = 0.55; P = 0.01**	**r = 0.47; P = 0.02**	r = -0.356; P = 0.19
PIIINP (µg/L)	**r = 0.46; P = 0.02**	**r = 0.45; P = 0.03**	r = 0.30; P = 0.13	r = -0.31; P = 0.27

TIMP-1: tissue inhibitor of metalloproteinase; MMP2: metalloproteinase matrix 2; PICP: carboxy terminal procollagen type 1 propeptide; CITP: C-terminal telopeptide of type 1 collagen; PIINP: N-terminal propeptide of type III procollagen
Bold indicates significant P value